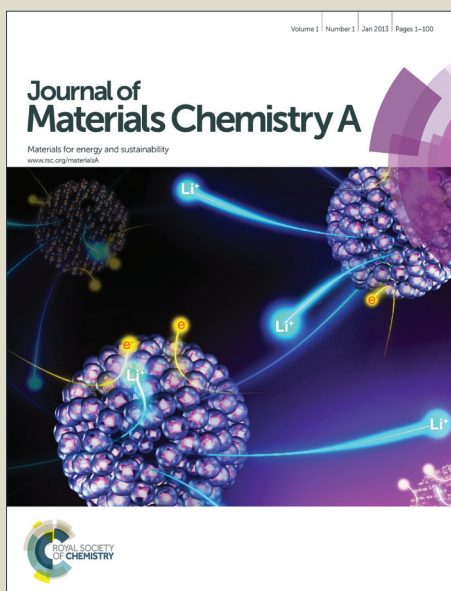


Journal of Materials Chemistry A

Accepted Manuscript



This is an *Accepted Manuscript*, which has been through the Royal Society of Chemistry peer review process and has been accepted for publication.

Accepted Manuscripts are published online shortly after acceptance, before technical editing, formatting and proof reading. Using this free service, authors can make their results available to the community, in citable form, before we publish the edited article. We will replace this *Accepted Manuscript* with the edited and formatted *Advance Article* as soon as it is available.

You can find more information about *Accepted Manuscripts* in the [Information for Authors](#).

Please note that technical editing may introduce minor changes to the text and/or graphics, which may alter content. The journal's standard [Terms & Conditions](#) and the [Ethical guidelines](#) still apply. In no event shall the Royal Society of Chemistry be held responsible for any errors or omissions in this *Accepted Manuscript* or any consequences arising from the use of any information it contains.

Innovative 3-D nanoforest heterostructure made of polypyrrole coated silicon nanotrees for new high performance hybrid micro-supercapacitor

David Aradilla,^{*a,b,c} Dorian Gaboriau,^{a,b,c,d} Gérard Bidan,^{a,c} Pascal
Gentile,^{*d,e} Maxime Boniface,^{d,e} Deepak Dubal,^f Pedro Gómez-Romero,^f Jan
Wimberg,^g Thomas J. S. Schubert,^g and Saïd Sadki ^{*a,b,c}

^aUniv. Grenoble Alpes, INAC-SPRAM, F-38000 Grenoble, France

^bCNRS, SPRAM, F-38000 Grenoble, France

^cCEA, INAC-SPRAM, F-38000 Grenoble, France

^dUniv. Grenoble Alpes, INAC-SP2M, F-38000 Grenoble, France

^eCEA, INAC-SP2M, F-38000 Grenoble, France

^fCIN2-CSIC. Campus UAB. Building Q, 08193 Bellaterra, Catalunya, Spain

^gIOLITEC Ionic Liquids Technologies GmbH, Salzstrasse 184, 74076 Heilbronn, Germany

*Corresponding author: david.aradilla@cea.fr, pascal.gentile@cea.fr and said.sadki@cea.fr

Abstract

In this work, an innovative 3-D symmetric micro-supercapacitor based on polypyrrole (PPy) coated silicon nanotree (SiNTr) hybrid electrodes has been fabricated. Firstly, SiNTrs were grown on silicon substrates by chemical vapor deposition (CVD) and then via an electrochemical method, the conducting polymer coating was deposited onto the surface of SiNTr electrodes. This study illustrates the excellent electrochemical performance of a hybrid micro-supercapacitor device using the synergistic combination between both PPy as electroactive pseudo-capacitive material and branched SiNWs as electric double layer capacitive material in the presence of an aprotic ionic liquid (N-methyl-N-propylpyrrolidinium bis(trifluoromethylsulfonyl)imide; PYR₁₃TFSI) as electrolyte. The hybrid device exhibited a specific capacitance as high as $\sim 14 \text{ mF cm}^{-2}$ and an energy density value of $\sim 15 \text{ mJ cm}^{-2}$ at a wide cell voltage of 1.5 V using a high current density of 1 mA cm^{-2} . Furthermore, a remarkable cycling stability after thousands of galvanostatic charge-discharge cycles with a loss of approximately 30% was obtained. The results reported in this investigation demonstrated that PPy coated SiNTr -based micro-supercapacitors exhibit the best performances among hybrid micro-supercapacitors made of silicon nanowire electrodes grown by CVD in terms of specific capacitance and energy density.

1. Introduction

Over the past years, the rapid and increasing demand of wearable and portable micro-electronic devices such as micro-electro-mechanical systems (MEMS), autonomous sensor networks, micro-robots, electronic biomedical implants (e.g. neuro-stimulators) or radio frequency identification (RFID) tags has triggered the development and design of high performance on-chip micro-electrochemical energy storage units for their integration into miniaturized devices.¹ Within this context, micro-supercapacitors (μ -SCs), as a novel family of micro power source device for energy harvesting, have aroused a special attention owing to their unique and interesting properties in terms of high power density, long lifespan, fast charge-discharge rate, excellent reversibility and high-frequency response.²

Currently, tremendous research efforts in the field of μ -SCs have been devoted to increase energy and power densities by developing novel nanostructured materials with high specific surface and advanced architectures. Thus, innovative materials based on nanostructured carbonaceous materials or derivatives have emerged as promising and prospective electro-active nanomaterials for micro-supercapacitor electrodes.³ Hence, μ -SCs based on onion-like carbon⁴, graphene⁵, carbon nanotubes⁶, carbide-derived carbon⁷ or diamond foam⁸ electrodes have drawn an enormous interest due to their excellent capacitive behavior, high reversibility, long cycling stability and wide operating temperature range. In spite of the important achievements focused on the investigation of nanostructured carbon materials, the development of ultra-high performance μ -SCs remains still a challenge.

From a material perspective, one dimensional (1D) nanostructured materials based on nanowires have attracted a great deal of attention in the field of μ -SCs.^{9,10} More specifically, silicon nanowires (SiNWs) have awakened a great potential for applications in the Si-based microelectronics industry due to their high compatibility with standard micro-fabrication processes and their integration into micro-electronic circuits, which involve important advantages compared with carbonaceous materials. Recently, the performance of SiNW-based μ -SCs have shown an excellent and quasi-ideal electrical double layer capacitive behavior employing different electrolytes such as organic solvents (e.g. a propylene carbonate PC solution containing 1M tetraethylammonium tetrafluoroborate),^{11,12} aprotic ionic liquids (EMIM-TFSI and PYR₁₃TFSI),¹³⁻¹⁵ protic ionic liquids (NEt₃H TFSI)¹⁶ or organic solvent-ionic liquid mixtures (PYR₁₃TFSI/PC).¹⁷ Accordingly, we have recently reported the excellent performance of a planar symmetric micro-supercapacitor device (e.g. 2-electrodes stacked) made of SiNW electrodes using a PYR₁₃TFSI aprotic ionic liquid as electrolyte. The results

reflected a wide operating cell voltage of 4V, a high maximal power density value of 182 mW cm⁻² as well as an excellent electrochemical stability after millions of galvanostatic charge-discharge cycles (e.g. 25 % of the initial capacitance was found to be lost).¹⁵ Nowadays, a new strategy in order to improve the capacitive properties of nanowires for μ -SC applications is focused on the concept of branched nanowires (known also as *nanotrees* or *nanoforest*).¹⁸ This approach is linked mainly with the enhancement of the developed active surface of electrodes, which is directly proportional to the specific capacitance (C). As a result, an improvement of both energy and power densities may be achieved. In recent years, several systems have already been reported using this principle as for example ZnO,¹⁹ Co₃O₄²⁰ nanowires or SiNWs.²¹ Precisely, silicon nanotrees (SiNTrs) have been employed as an excellent electrodes for micro-supercapacitor devices in our previous work.²¹ Thus, μ -SCs based on SiNTrs exhibited a C value of 84 μ F cm⁻². This value was found to be higher than SiNW-based μ -SC (C: 23 - 50 μ F cm⁻²),^{15,22} demonstrating the potential of branched nanowires as advanced electrodes for electrochemical energy storage devices.

As it was aforementioned, the development of new nanostructured materials will play a crucial role on the design of ultra-high performance μ -SCs. Concerning this research activity, in recent years various types of pseudo-capacitive materials such as transition metal oxides (e.g. NiO),^{23,24} metal hydroxides (e.g. Ni(OH)₂),²⁵ or conducting polymers (e.g. poly(3,4-ethylenedioxythiophene) PEDOT)^{26,27} have been successfully deposited on SiNWs by means of electrochemical methods. Regarding their working principle, hybrid micro-pseudocapacitors store charge through faradaic or redox reactions associated with charge transfer processes, which occur at the surface of the electrodes. Therefore, they are able to deliver higher volumetric capacitance and energy density than electric double layer μ -SCs.²⁸ In this way, the synergistic effect produced between branched nanowires and pseudo-capacitive materials could open a new scenario in the field of new high performance hybrid micro-supercapacitors. Within this context, branched nanowires functionalized by transition metal oxides (e.g. MnO₂) were reported as promising supercapacitor electrodes.²⁹ However, to the best of our knowledge no work has been reported dealing with the deposition of conducting polymers, as pseudo-capacitive material, on branched nanowires and more specifically on SiNTrs.

Herein, we originally report the excellent performance of a novel high performance 3-D μ -SC device based on polypyrrole (PPy) coated SiNTr hybrid electrodes using PYR₁₃TFSI aprotic ionic liquid as electrolyte. The electrochemical characterization of the device was evaluated by cyclic voltammetry, galvanostatic charge-discharge cycles and electrochemical

impedance spectroscopy. Furthermore, a morphological characterization of the hybrid electrodes was examined by scanning, transmission and focus ion beam electron microscope.

2. Experimental section

Materials and reagents. Highly p-doped Si (111) substrates (doping level: $5 \cdot 10^{18}$ doping atoms cm^{-3}) and resistivity less than $0.005 \Omega \text{ cm}$ were used as the substrate for SiNTr growth. Pyrrole and silver trifluoromethanesulfonate were purchased from Sigma-Aldrich. N-methyl-N-propylpyrrolidinium bis(trifluoromethylsulfonyl)imide was purchased from IOLITEC (Ionic Liquids Technologies GmbH, Germany) and used without further purification. Pyrrole was distilled before previous electrochemical experiments.

Growth of SiNTrs. Highly doped SiNTr electrodes with a length of approximately $50 \mu\text{m}$ were grown in a CVD reactor (EasyTube3000 First Nano, a Division of CVD Equipment Corporation) by using the vapor-liquid-solid (VLS) method via gold catalysis on highly doped p-Si (111) substrate using an optimal deposition procedure, which has been previously detailed.²¹ Briefly, the trunks were grown from a 4 nm evaporated thin gold film performed at 600°C , under 6 Torr total pressure, with 40 sccm (standard cubic centimeters) of SiH_4 , 100 sccm of B_2H_6 gas (0.2% B_2H_6 in H_2) for p doping, 100 sccm of HCl gas and 700 sccm of H_2 as supporting gas. Prior to the second gold catalyst, gold was removed using a I_2 and KI solution followed by a deoxidation in a 10% HF solution in order to remove the thin native oxide layer formed after the trunk growth. After that, the branches were grown from a 1 nm evaporated gold thin film at 600°C , under 6 Torr total pressure, with 50 sccm of SiH_4 , 100 sccm of B_2H_6 gas (0.2% B_2H_6 in H_2), 100 sccm of HCl gas and 500 sccm of H_2 as carrier gas.

Electropolymerization of Py on SiNTrs. PPy films were electrochemically deposited from a PYR_{13} TFSI solution containing 0.1 M Py as the monomer using an AUTOLAB PGSTAT 302 N potentiostat-galvanostat. The electropolymerization was conducted in a 3-electrode electrochemical cell. SiNTrs were employed as the working electrode, a Pt wire was used as the counter electrode and the nonaqueous Ag/Ag^+ reference electrode was composed of a silver wire immersed in a 10 mM silver trifluoromethanesulfonate (AgTf) solution in PYR_{13} TFSI. The electrochemical deposition of Py was carried out by potentiostatic methods using a constant potential of 0.4 V (vs Ag/Ag^+) under a polymerization charge of 750 mC cm^{-2} controlled by the chronocoulometry technique in an argon-filled glove box with oxygen and water levels less than 1 ppm. After the electrochemical deposition, the electrodes were washed in acetone and dried with a N_2 flow before the electrochemical characterization. The PPy mass was estimated by subtracting the difference before and after electrodeposition on SiNTrs using a METTLER Toledo balance (precision of 0.01 mg). A total mass of $2.7 \cdot 10^{-4} \text{ g}$ was identified for each electrode.

Morphological characterization. The morphology of the resulting SiNTr and hybrid SiNTr electrodes was examined by scanning, transmission and focus ion beam (FIB) electron microscopy. A Zeiss Ultra 55 scanning microscope operating at an accelerating voltage of 3 kV was used. For TEM characterization, samples were prepared by drop-casting a solution containing PPy-coated SiNTrs in water on a copper grid. TEM images were carried out using a FEI Osiris microscope at a voltage of 200 kV. FIB measurements were conducted by a STRATA 400A microscope at a voltage of 16 kV using a current of 1.4 nA.

Fabrication and electrochemical characterization of the hybrid micro-supercapacitor. Symmetric micro-supercapacitors were designed from hybrid nanostructured electrodes made of PPy-coated SiNTrs as mentioned in the previous section. A homemade two-electrode supercapacitor cell was built by assembling two hybrid nanostructured electrodes separated by a Whatman glass fiber paper separator soaked with the electrolyte (PYR₁₃ TFSI). Cyclic voltammetry (CV), galvanostatic charge-discharge cycles and electrochemical impedance spectroscopy (EIS) were performed using a multichannel VMP3 potentiostat/galvanostat with Ec-Lab software (Biologic, France). EIS measurements were performed using a sinusoidal signal of ±10 mV amplitude and a frequency range from 400 kHz to 10 mHz. All measurements were carried out using PYR₁₃TFSI as electrolyte in an argon-filled glove box with oxygen and water levels less than 1 ppm at room temperature.

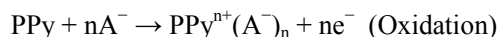
The specific capacitance values of the device were calculated from the charge-discharge curves using the following equation $C = i/A(dV/dt)$, where the i is the discharge current, A is the area of the electrode (1 cm²) and dV/dt corresponds to the slope of discharging curve. The energy density (E) and power density (P) are calculated by using $E=0.5C(\Delta V)^2$ and $P=E/t$, where ΔV is the potential range and t is the total time of discharge.

3. Results and discussion

The morphology of SiNTr and PPy-coated SiNTr electrodes was analyzed by scanning electron microscopy as displayed in Figure 1 (a-d). Figure 1a shows the cross sectional view of SiNTrs grown by CVD on silicon substrates. As can be seen, the length of SiNTrs was estimated to be $\sim 50 \mu\text{m}$. The density of SiNWs (trunks) was determined to be $3 \cdot 10^9$ nanowires per cm^2 with a diameter ranged from 20 to 500 nm according to our previous work.²¹ Figure 1b illustrates the formation of branches on SiNWs (SiNTrs) with the following characteristics: length of $\sim 2 \mu\text{m}$ and diameter ranged from 20 up to 70 nm, which were reported also in our recent study.²¹ The functionalization of SiNTr electrodes using PPy as pseudo-capacitive material was carried out using an electrochemical deposition (Fig 1c and 1d). Thus, Py was deposited electrochemically on SiNTrs using a potentiostatic method at a constant potential of 0.4 V. This optimal oxidation potential was found in excellent agreement with those results concerning the electrochemical deposition of PEDOT on SiNWs (0.4 V vs Ag/Ag⁺).²⁶ As a result, a uniform and homogeneous PPy coating was deposited onto SiNTrs with a globular morphology as illustrated in Figure 1c. Accordingly, a cross sectional view of the hybrid electrode was shown in Figure 1d reflecting again a successfully deposition of PPy on SiNTrs. In order to corroborate this information, a more detailed morphological characterization of the hybrid electrodes was performed by FIB and TEM microscopy. A FIB microscopy image of the hybrid nanostructure is displayed in Figure 2e. According to this figure, the deposition of PPy onto SiNWs (trunks) exhibits a thickness of ~ 100 nm. This value was found to be in excellent agreement with similar works using conducting polymers deposited on nanowires in the field of energy storage devices. Thus, a thin layer of PEDOT was deposited on SiNWs for its use as battery anode (thickness ~ 100 nm)²⁷ or as micro-supercapacitor electrode (thickness ~ 300 nm)²⁶ with excellent electrochemical performances. From this perspective, a nanometric thickness was considered appropriate in this study. Accordingly, Figure 2f shows a high-resolution TEM image of a PPy-coated SiNW corresponding to the branch. As can be seen, a thickness of the conducting polymer coating was determined to be around 20 nm. Consequently, these results reveal the success of the chronocoulometry technique to produce hybrid electrodes based on conducting polymer-coated SiNTrs with a nanometric thickness.

The electrochemical performance of a PPy-coated SiNTr electrode was evaluated by CV technique using a three-electrode cell in a PYR₁₃TFSI solution. Figure 2a presents typical CV curves of the hybrid electrode at different scan rates of 5, 10 and 20 mVs^{-1} recorded in the potential range from -1.5 to 0.5 V. As can be observed, a pair of oxidation-reduction peaks

were detected, which are associated with the oxidation and reduction of polypyrrole. The reduction peak is ascribed with the de-intercalation of anion (TFSI⁻) from the PPy film due to the reduction of the polymer from the oxidized to the neutral state, whereas the oxidation peak reflects the intercalation of anions into the polymeric structure. The corresponding chemical processes are described according to the following reactions:



This electrochemical behavior has been reported recently in a previous work using 1-butyl-1-methylpyrrolidinium bis(trifluoromethanesulfonyl)imide as electrolyte. In this particular case, PPy was synthesized on Pt disks using the same electrolyte.³⁰ Within this context, similar micro-supercapacitor systems based on nanowires functionalized by pseudocapacitive materials, as for example MnO₂ coated Co₃O₄ nanowires, showed the same electrochemical tendency (two redox peaks) using aqueous electrolytes.³¹ In this way, the faradaic reactions observed in this study suggest that the specific capacitance of PPy-coated SiNTrs is mainly contributed to the pseudo-capacitive behaviour induced by the conducting polymer at the electrode/electrolyte surface. This electrochemical behaviour was found to be different from those systems based on bare SiNW and SiNTr electrodes, where only an electrical double layer capacitance (e.g. quasi-rectangular voltammetric curves) was observed as reported previously.^{15,16,21} The plot displayed in Figure 2a shows also no shape change with increase of scan rate (from 5 up to 20 mVs⁻¹) implying that PPy-coated SiNTr electrodes possess a high current capability and good rate performance. Moreover, the faradaic peak potential of the hybrid electrode shifts with the increase of the scan rate maintaining a good reversibility. Figure 2b and 2c show the electrochemical performance of the hybrid planar micro-supercapacitor device (2-electrodes stacked) examined by CV. Regarding Figure 2b, a representative CV curve of the hybrid device was recorded at a scan rate of 5 mVs⁻¹ within a large potential window of 1.5 V. This potential was chosen as an optimal voltage according to our previous works reported in the literature concerning the electrochemical performance of micro-supercapacitors based on SiNTr and PEDOT-coated SiNW electrodes.^{21,26} The curve shows a near symmetric rectangular shape and good reversibility in the current response on voltage reversal, implying an excellent behaviour. According to the figure 2b, it is possible to observe again the clear improvement of the capacitive properties induced by the PPy coating compared with bare SiNTrs. At low scan rates (5 mV s⁻¹), the faradaic contribution of the conducting polymer on the hybrid electrodes keeps an extraordinary capacitive performance.

Nevertheless, the CV curve of the hybrid device at high scan rates (300 mV s^{-1}) presented a deformation of the shape compared to Figure 2b because of the kinetically limited pseudocapacitive reactions (Figure 2c). It should be noted that the rectangular shape of the curve was retained demonstrating the high potential of this material as a hybrid micro-supercapacitor. This tendency was also corroborated in our previous study dealing with the deposition of PEDOT on SiNWs for hybrid micro-supercapacitors.²⁶ The electrochemical properties of the hybrid device were also investigated using galvanostatic charge-discharge measurements. Figure 2d shows the galvanostatic charge-discharge cycles using a high current density of 1 mA cm^{-2} at a voltage window of 1.5V. From figure 2d, it is clearly seen that the cycles reflect symmetric and linear profiles revealing an excellent capacitive behaviour and highly reversibility. A specific capacitance value of $\sim 14 \text{ mF cm}^{-2}$ (52 Fg^{-1}) was calculated, which represents an important enhancement compared with other values reported in the literature employing μ -SCs based on nanostructured carbonaceous materials. Thus, interdigitated on-chip micro-supercapacitors based on carbide derived carbon films, onion-like carbon, graphene or multi-walled carbon nanotubes (MWNTs) exhibited a specific capacitance value ranged from 1 up to 3 mF cm^{-2} respectively.³²⁻³⁵ More recently, symmetrical activated carbon -based EDLCs using an ionogel as electrolyte have shown similar capacitance values (15 mF cm^{-2}) by comparison in this work.³⁶ Figure 2e displays the variance of the areal specific capacitance versus current density where specific capacitance reached a plateau for current densities higher than 0.5 mA cm^{-2} . The specific capacitance values were ranged from 14.5 mF cm^{-2} (0.1 mA cm^{-2}) up to 13.7 mF cm^{-2} (1 mA cm^{-2}) respectively.

EIS measurement is an important tool in order to determine the capacitive behaviour as well as the electrode-electrolyte interface of a μ -SC device. Figure 3a shows the corresponding Nyquist plot obtained for the hybrid micro-supercapacitor device over the frequency range from 400 kHz to 0.01 Hz. The amplification of high-frequency region is shown in the inset. As can be seen, two main different regions were observed, a semi-circle in high frequency region represents the charge transfer resistance (R_{ct}) caused by faradaic reactions and a nearly vertical plot at low frequency indicating an ideal capacitive behaviour. Accordingly, the Bode plot represented in Figure 3b showed that at 10 mHz the phase angle of the micro-supercapacitor corresponds to $\sim 85^\circ$, close to 90° for ideal capacitors. Figure 3c displays the evolution of C'' versus frequency for the micro-supercapacitor in order to calculate the relaxation time constant of the device (τ_0).³⁷ This parameter is defined as the minimum time needed to discharge all the energy from the device with an efficiency of more

than 50%.⁴ From the plot displayed in Figure 3c, the relaxation time constant was calculated using the following relation ($\tau_0 = 1/f$), which was determined to be 2.2s. This value was found shorter than other supercapacitors based on meso- and micro-porous composite carbons reported in the literature ($\tau_0 = 18$ s).³⁸ Nevertheless, it is worth noting that the value of relaxation time constant of our device was found also to be in the same order of magnitude than those micro-supercapacitors based on activated carbon ($\tau_0 = 0.7$ s).⁴ or functionalized nanostructured carbon using pseudo-capacitive materials such as transition metal oxides (e.g. MWNT/V₂O₅ or MWNT/MnO₂; $\tau_0 = 0.2 - 0.4$ s).^{39,40} Based on these results, the hybrid device reported in this investigation exhibits an outstanding power response ability.

The Ragone plot in Figure 4a depicts the energy density (mJ cm^{-2}) and power density (mW cm^{-2}) of the hybrid μ -SCs studied in this work, more specifically PPy coated SiNW and SiNTr – based μ -SCs. The results in Figure 4a demonstrate that the functionalization of SiNTrs exhibits better capacitive properties than functionalized SiNWs, evidencing the enhancement of the performance owing to their hyper-nanostructuration, which leads to higher active surface. Recently, we have described a new hybrid μ -SC based on PEDOT-coated SiNWs with interesting capacitive properties in terms of high energy density (E : 9 mJ cm^{-2}) and specific capacitance (C : 8 mF cm^{-2}).²⁶ These values have been compared with the results presented in this investigation. Accordingly, PPy-coated SiNTr μ -SCs have exhibited an amazing improvement of the specific capacitance and energy density compared with PEDOT or PPy-coated SiNW μ -SCs. Thus, the former showed a C (14 mF cm^{-2}) and E density (15 mJ cm^{-2}) values higher than the latter (C : 10 mF cm^{-2} and E : 11 mJ cm^{-2}) at high current densities (e.g. 1 mA cm^{-2}) as shown in Figure 4a. Therefore, the results obtained in this study evidence the synergistic effect produced between the hybrid electrodes made of PPy-coated SiNTrs and PYR₁₃TFSI as electrolyte, with an improvement of 40 % compared with functionalized SiNWs. Figure 4b describes the performance of hybrid micro-supercapacitors based on silicon nanowires grown by CVD such as PEDOT/SiNWs,²⁶ Diamond/SiNWs,¹⁷ SiC/SiNWs,⁴¹ or Ni(OH)₂/SiCNWs.²⁵ In addition, other micro-supercapacitors based on nanostructured carbonaceous materials as for example carbon nanotubes,^{6,42} graphene⁴³ or pseudocapacitive materials: (RuO₂ nanorods),⁴⁴ have been also reported. Regarding Figure 4b, PPy-coated SiNTr μ -SCs exhibit the highest energy density (15 mJ cm^{-2}) and one of the best performance in terms of power density (0.8 mW cm^{-2}). As a result, this novel hybrid micro-supercapacitor with high energy and power densities represents an alternative and promising approach to the conventional micro-supercapacitors based on silicon nanowires or carbonaceous materials.

Another important index of a micro-supercapacitor concerns its long-term stability. Particularly, in this work the cycling stability of the devices was evaluated by repeating successive galvanostatic charge-discharge cycles at a high current density of 1 mA cm^{-2} in a wide cell voltage of 1.5 V. As displayed in Figure 5a, SiNTr and SiNW-based micro-supercapacitors exhibited practically any loss of electrochemical stability after 10 000 galvanostatic charge-discharge cycles. Thereby, micro-supercapacitors based on SiNW and SiNTr electrodes showed the same cycling stability. However, the electrochemical deposition of PPy on SiNTr electrodes reflected that the hybrid device retained 70% of its initial capacitance, indicating a good cycling stability. This difference can be explained by the charge storage mechanism associated for each system. Micro-supercapacitors based on SiNT electrodes store energy by electrostatic charge accumulation at electrode/electrolyte interfaces, involving no transfer of charge associated with non-faradaic reactions. Accordingly, charge storage in this kind of systems allows to achieve very high cycling stabilities (up to millions of cycles with a loss of only 2% of its initial capacitance).²¹ In contrast, hybrid micro-supercapacitors based on PPy coated SiNTr electrodes storage charge faradaically through the transfer of charge between the electrode and electrolyte (faradaic reactions, Figure 2a). The faradaic processes involve in this energy storage mechanism lead to obtain greater capacitance and energy densities than SiNTr micro-supercapacitors, although the cycling stability is lower (thousands of cycles). Nevertheless, the lifetime of this hybrid device was found higher than other micro-supercapacitors based on pseudo-capacitive materials as for examples MnO_2 or PPy. Thus, the cyclic performance of μ -SCs based on nanostructured MnO_2 electrodes onto Si wafers showed a loss of $\sim 27\%$ after 1000 galvanostatic cycles,⁴⁵ or 56% for μ -SCs based on three dimensional interdigital PPy/C-MEMS electrodes.⁴⁶ More recently, other supercapacitors based on PPy shell@3-D Ni metal core structured electrodes or using composites of PPy and MnO_2 exhibited similar cycling stabilities compared with the results obtained in this work (electrochemical stability loss of 20% after 5000 cycles).^{47,48} The morphology of PPy-coated SiNTrs after cycling was examined by using SEM images according to Figure 5b. As illustrated, the structure of the hybrid electrode remained unchanged even after thousands of successive charge-discharge cycles presenting an excellent structural stability, comparable to those observed in Figure 1c and 1d corresponding to PPy-coated SiNTrs as grown (e.g. not cycled in an electrochemical device).

4. Conclusions

In summary, the development and design of an innovative micro-supercapacitor made of PPy-coated SiNTr electrodes using a $\text{PYR}_{13}\text{TFSI}$ aprotic ionic liquid as electrolyte has been successfully tested. Among the various types of hybrid micro-supercapacitors based on silicon nanowires grown by CVD reported in the literature, PPy-coated SiNTrs based micro-supercapacitors present one of the best electrochemical performance in terms of specific capacitance (C : 14 mF cm^{-2}), energy (E : 15 mJ cm^{-2}) and power (P : 0.8 mW cm^{-2}) densities. In addition, the device shows a remarkable electrochemical stability with a loss of specific capacitance of 30% after 10000 galvanostatic charge-discharge cycles compared with other functionalized hybrid micro-supercapacitors. Consequently, this work demonstrates that this hybrid symmetric micro-supercapacitor has promising potential in application of energy storage devices, specifically for on-chip advanced electrochemical micro-supercapacitors.

Acknowledgements

This project has received funding from the European Union's Seventh Program for Research, Technological Development and Demonstration under Grant agreement no. 309143 (2012–2015). Dorian Gaboriau thanks the 'Délégation Générale pour l'Armement' (DGA) and the CEA for financial support.

References

- 1 C. Meng, J. Maeng, S. W. M. John and P. P. Irazoqui, *Adv. Energy Mater.*, 2014, **4**, 1301269.
- 2 M. Beidaghi and Y. Gogotsi, *Energy Environ. Sci.*, 2014, **7**, 867.
- 3 X. Lia and B. Weia, *Nano Energy*, 2013, **2**, 159.
- 4 D. Pech, M. Brunet, H. Durou, P. Huang, V. Mochalin, Y. Gogotsi, P.-L. Taberna and P. Simon, *Nat. Nanotechnology*, 2010, **5**, 651.
- 5 G. Xiong, C. Meng, R. G. Reifengerger, P. P. Irazoqui and T. S. Fisher, *Electroanalysis*, 2014, **26**, 30.
- 6 B. Hsia, J. Marschewski, S. Wang, J. Bin, C. Carraro, D. Poulidakos, C. P. Grigoropoulos and R. Maboudian, *Nanotechnology*, 2014, **25**, 055401.
- 7 J. Chmiola, C. Largeot, P.-L. Taberna, P. Simon and Y. Gogotsi, *Science*, 2010, **328**, 480.
- 8 F. Gao, M. T. Wolfer and C. E. Nebel, *Carbon*, 2014, **80**, 833.
- 9 L. Mai, X. Tian, X. Xu, L. Chang and L. Xu, *Chemical Reviews*, 2014, **114**, 11828.
- 10 K.-Q. Peng, X. Wang, L. Li, Y. Hu and S.-T. Lee, *Nano Today*, 2013, **8**, 75.
- 11 F. Thissandier, A. Le Comte, O. Crosnier, P. Gentile, G. Bidan, E. Hadji, T. Brousse and S. Sadki, *Electrochem. Commun.*, 2012, **25**, 109.
- 12 F. Thissandier, N. Pauc, T. Brousse, P. Gentile and S. Sadki, *Nanoscale Research Lett.*, 2013, **8**, 38.
- 13 F. Thissandier, L. Dupré, P. Gentile, T. Brousse, G. Bidan, D. Buttard and S. Sadki, *Electrochim. Acta*, 2014, **117**, 159.
- 14 J. P. Alper, S. Wang, F. Rossi, G. Salvati, N. Yiu, C. Carraro and R. Maboudian, *Nano Lett.*, 2014, **14**, 1843.
- 15 D. Aradilla, P. Gentile, G. Bidan, V. Ruiz, P. Gomez-Romero, T. J. S. Schubert, H. Sahin, E. Frackowiak and S. Sadki, *Nano Energy*, 2014, **9**, 273.
- 16 D. Aradilla, P. Gentile, V. Ruiz, P. Gomez-Romero, J. Wimberg, B. Iliev, T. J. S. Schubert, S. Sadki and G. Bidan, *Adv. Nat. Sci: Nanosci. Nanotechnol.*, 2015, **6**, 015004.
- 17 F. Gao, G. Lewes-Malandrakis, M. T. Wolfer, W. Müller-Sebert, P. Gentile, D. Aradilla, T. Schubert and C. E. Nebel, *Diamond and Related Materials*, 2015, **51**, 1.
- 18 C. Cheng and H. J. Fan, *Nano Today*, 2012, **7**, 327.
- 19 X. Sun, Q. Li, Y. Lu and Y. Mao, *Chem. Commun.*, 2013, **49**, 4456.

- 20 G. Zhang, T. Wang, X. Yu, H. Zhang, H. Zhang, H. Duann and B. Lu, *Nano Energy*, 2013, **2**, 586.
- 21 F. Thissandier, P. Gentile, T. Brousse, G. Bidan and S. Sadki, *J. Power Sources*, 2014, **269**, 740.
- 22 F. Thissandier, P. Gentile, N. Pauc, E. Hadji, A. Le Comte, O. Crosnier, G. Bidan, S. Sadki and T. Brousse, *Electrochem.*, 2013, **81**, 777.
- 23 B. Tao, J. Zhang, F. Miao, S. Hui and L. Wan, *Electrochim. Acta*, 2010, **55**, 5258.
- 24 F. Lu, M. Qiu, X. Qi, L. Yang, J. Yin, G. Hao, X. Feng, J. Li and J. Zhong, *Appl. Phys A*, 2011, **104**, 545.
- 25 L. Gu, Y. Wang, R. Lu, W. Wang, X. Peng and J. Sha, *J. Power Sources*, 2015, **273**, 479.
- 26 D. Aradilla, G. Bidan, P. Gentile, P. Weathers, F. Thissandier, V. Ruiz, P. Gomez-Romero, T. J. S. Schubert, H. Sahin and S. Sadki, *RSC Adv.*, 2014, **4**, 26462.
- 27 Y. Yao, N. Liu, M. T. McDowell, M. Pasta and Y. Cui, *Energy Environ. Sci.*, 2012, **5**, 7927.
- 28 G. Yua, X. Xieb, L. Pand, Z. Boad and Y. Cui, *NanoEnergy*, 2013, **2**, 213.
- 29 R. Zou, M. F. Yuen, Z. Zhang, J. Hu and W. Zhang, *J. Mater. Chem. A*, 2015, **3**, 1717.
- 30 L. Viau, J. Y. Hihn, S. Lakard, V. Moutarlier, V. Flaud and B. Lakard, *Electrochim. Acta*, 2014, **137**, 298.
- 31 J. Liu, J. Jiang, C. Cheng, H. Li, J. Zhang, H. Gong and H. J. Fan, *Adv. Mater.*, 2011, **23**, 2076.
- 32 P. Huang, M. Heon, D. Pech, M. Brunet, P.-L Taberna, Y. Gogotsi, S. Lofland, J. D. Hettinger and P. Simon, *J. Power Sources*, 2013, **225**, 240.
- 33 P. Huang, D. Pech, R. Lin, J. K. McDonough, M. Brunet, P.-L Taberna, Y. Gogotsi and P. Simon, *Electrochem. Commun.*, 2013, **36**, 53.
- 34 T. Mai Dinh, K. Armstrong, D. Guayc and D. Pech, *J. Mater. Chem. A*, 2014, **2**, 7170.
- 35 M. Beidaghi and C. Wang, *Adv. Funct. Mater.*, 2012, **22**, 4501.
- 36 M. Brachet, T. Brousse and J. Le Bideau, *ECS Electrochemistry Lett.*, 2014, **3**, A112.
- 37 P. L. Taberna, P. Simon and J. F. Fauvarque, *J. Electrochem. Soc.*, 2003, **150**, A292.
- 38 J. Yin, D. Zhang, J. Zhao, X. Wang, H. Zhub and C. Wang, *Electrochim. Acta*, 2014, **136**, 504.
- 39 G. Lee, D. Kim, J. Yun, Y. Ko, J. Cho and J. S. Ha, *Nanoscale*, 2014, **6**, 9655.
- 40 D. Kim, J. Yun, G. Lee and J. S. Ha, *Nanoscale*, 2014, **6**, 12034.

- 41 J. P. Alper, M. Vincent, C. Carraro and R. Maboudian, *Appl. Phys. Lett.*, 2012, **100**, 163901.
- 42 D. Membreno, L. Smith, K. S. Shin, C. O. Chui and B. Dunn, *Transl. Mater. Res.*, 2015, **2**, 015001.
- 43 J. J. Yoo, K. Balakrishan, J. Huang, V. Meunier, B. G. Sumpter, A. Srivastava, M. Conway, A. L. M. Reddy, J. Yu, R. Vajtaj and P. M. Ajayan, *Nano Lett.*, 2011, **11**, 1423.
- 44 C.-C. Liu, D.-S. Tsai, D. Susanti, W.-C. Yeh, Y.-S. Huang and F.-J. Liu, *Electrochim. Acta*, 2010, **55**, 5768.
- 45 X. Wang, B. D. Myers, J. Yan, G. Shekhawat, V. Dravid and P. S. Lee, *Nanoscale*, 2013, **5**, 4119.
- 46 M. Beidaghi and C. Wang, *Electrochim. Acta*, 2011, **56**, 9508.
- 47 G. -F. Chen, Y.-Z. Su, P.-Y. Kuang, Z.-Q. Liu, D.-Y. Chen, X. Wu, N. Li and S.-Z. Qiao, *Chem. Eur. J.*, 2015, **21**, 4614.
- 48 G.-F. Chen, Z.-Q. Liu, J.-M. Lin, N. Li and Y.-Z. Su, *J. Power Sources*, 2015, **273**, 479.

Captions to Figures

Figure 1. Scanning electron micrographs of a) Cross sectional view of SiNTrs. b) Branches grown on SiNW trunks. c) PPy coated SiNTrs at 45° title angle (Top view). Inset shows a magnified image. Scale bar: 100 nm and d) Cross sectional view of PPy coated SiNTrs. e) FIB measurement of a PPy-coated SiNW (trunk). f) TEM image of a PPy-coated SiNW (branch).

Figure 2. a) CV curves of a PPy coated SiNTr electrode at different scan rates (5, 10 and 20 mVs⁻¹ respectively) in a 3-electrochemical cell. Initial and final potential: -1.5 V; reversal potential: 0.5 V b) CV curves of a PPy coated SiNTr micro-supercapacitor (green line) and SiNTr micro-supercapacitor (blue line) on silicon substrates with the same scan rate of 5 mV s⁻¹. Inset shows the magnified plot of the SiNTr micro-supercapacitors. c) CV curve of a PPy coated SiNTr micro-supercapacitor at a high scan rate of 300 mVs⁻¹. d) Galvanostatic charge-discharge cycles of the hybrid device recorded at a current density of 1 mA cm⁻² using a cell voltage of 1.5 V. e) Specific capacitance versus current density (0.1 – 1 mA cm⁻²)

Figure 3. a) Nyquist plot of the hybrid device measured at 0V using a frequency range from 400 kHz to 10 mHz. Inset shows magnified high frequency region. b) Bode plot of the hybrid micro-supercapacitor. c) Evolution of the imaginary capacitance versus frequency using the conditions described in a). The relaxation time (τ_0) of the device is indicated in the plot using an arrow.

Figure 4. a) The Ragone plot of hybrid micro-supercapacitors based on conducting PPy coated SiNWs (blue squares) and PPy coated SiNTrs (purple diamonds) calculated by varying the discharging current density from 0.1 to 1 mA cm⁻² at a potential window of 1.5 V. b) Comparison of the PPy-coated SiNTr hybrid micro-supercapacitor with state-of-the art hybrid micro-supercapacitors based on silicon nanowires grown by CVD and other carbonaceous and pseudocapacitive materials.

Figure 5. a) Cycling stability of micro-supercapacitors performed using 10000 complete galvanostatic charge-discharge cycles at a current density of 1 mA cm⁻² between 0 and 1.5 V using nanostructured Si (SiNWs and SiNTrs; blue line) and PPy-coated SiNTr (green line) electrodes. b) SEM micrograph of PPy coated SiNTrs after cycling under the conditions described in a) at 45° tilted angle.

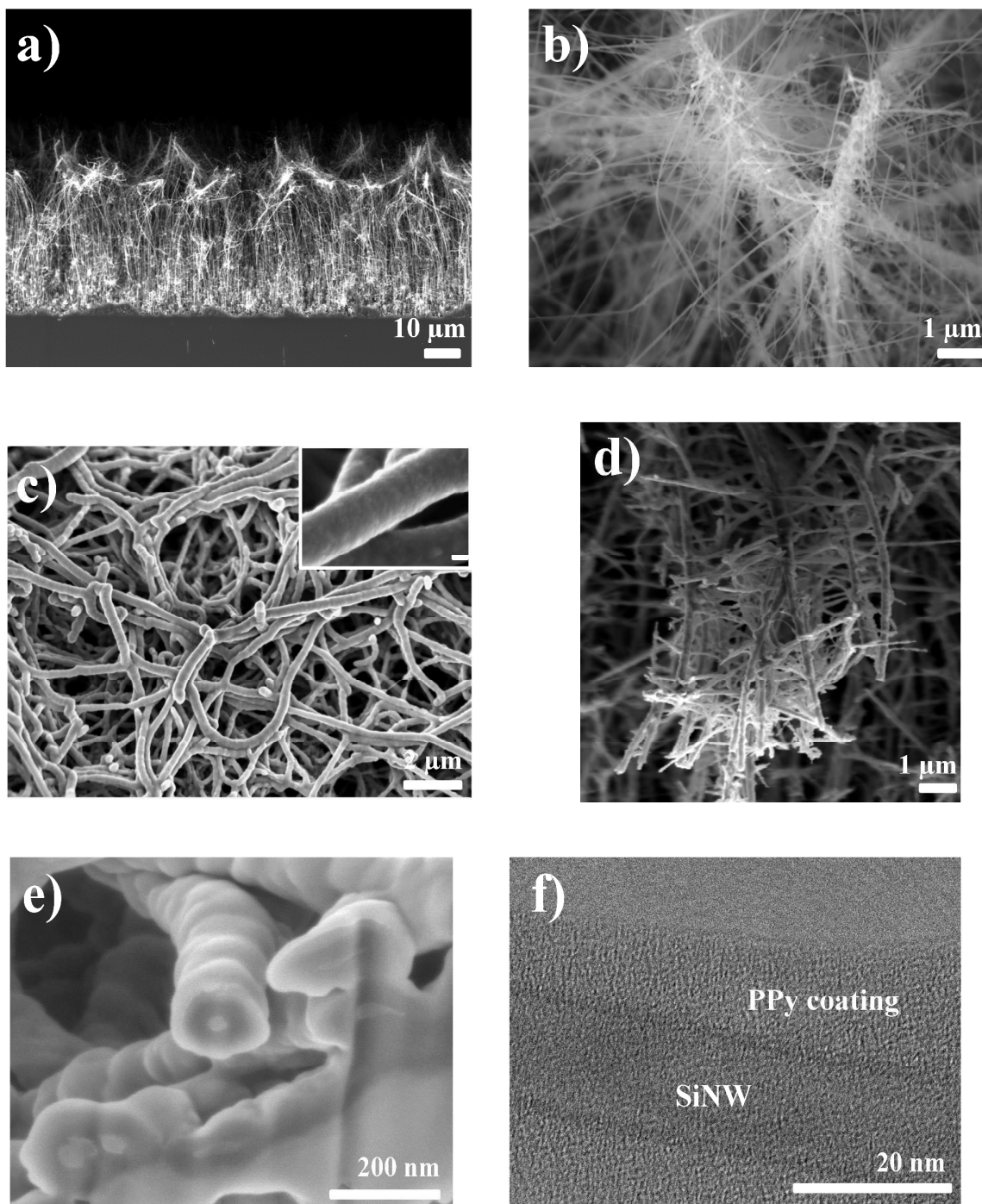


Figure 1

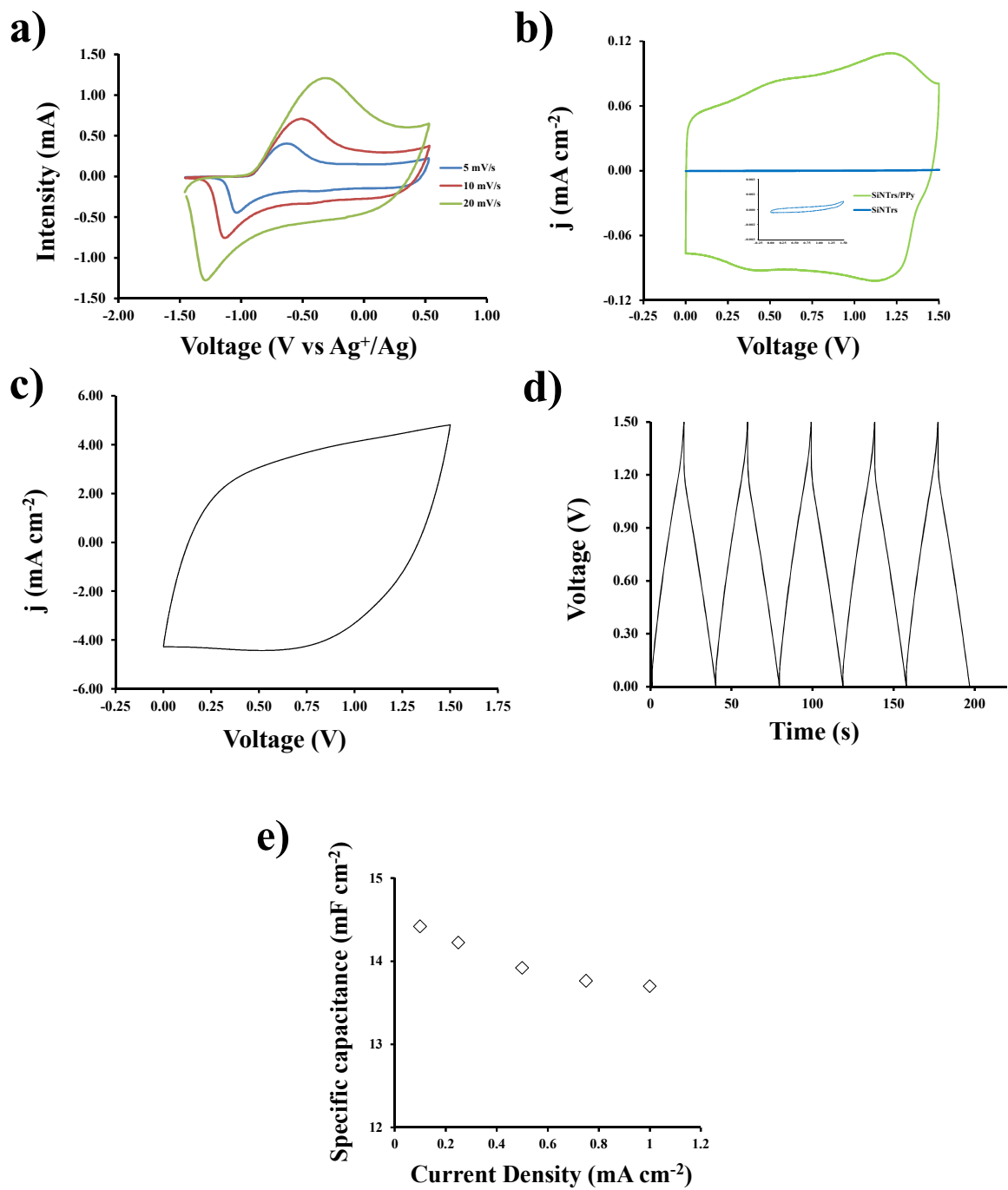
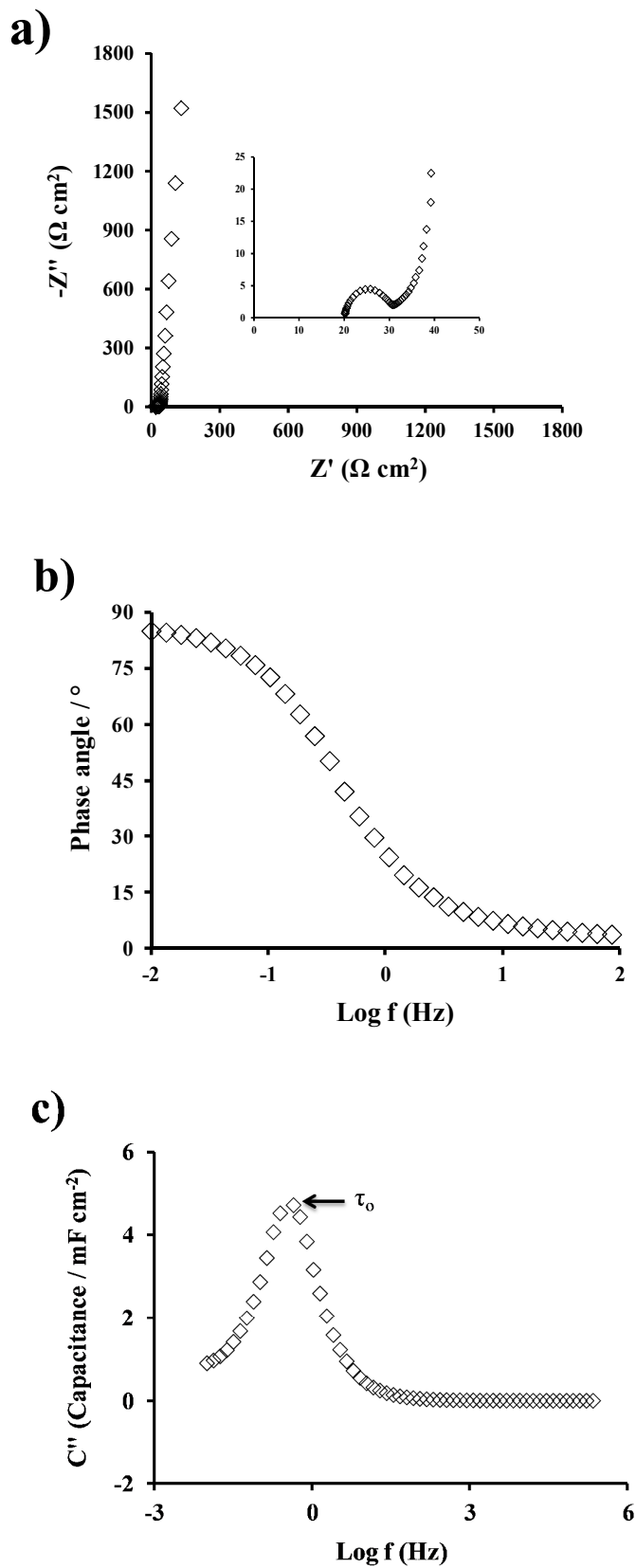


Figure 2



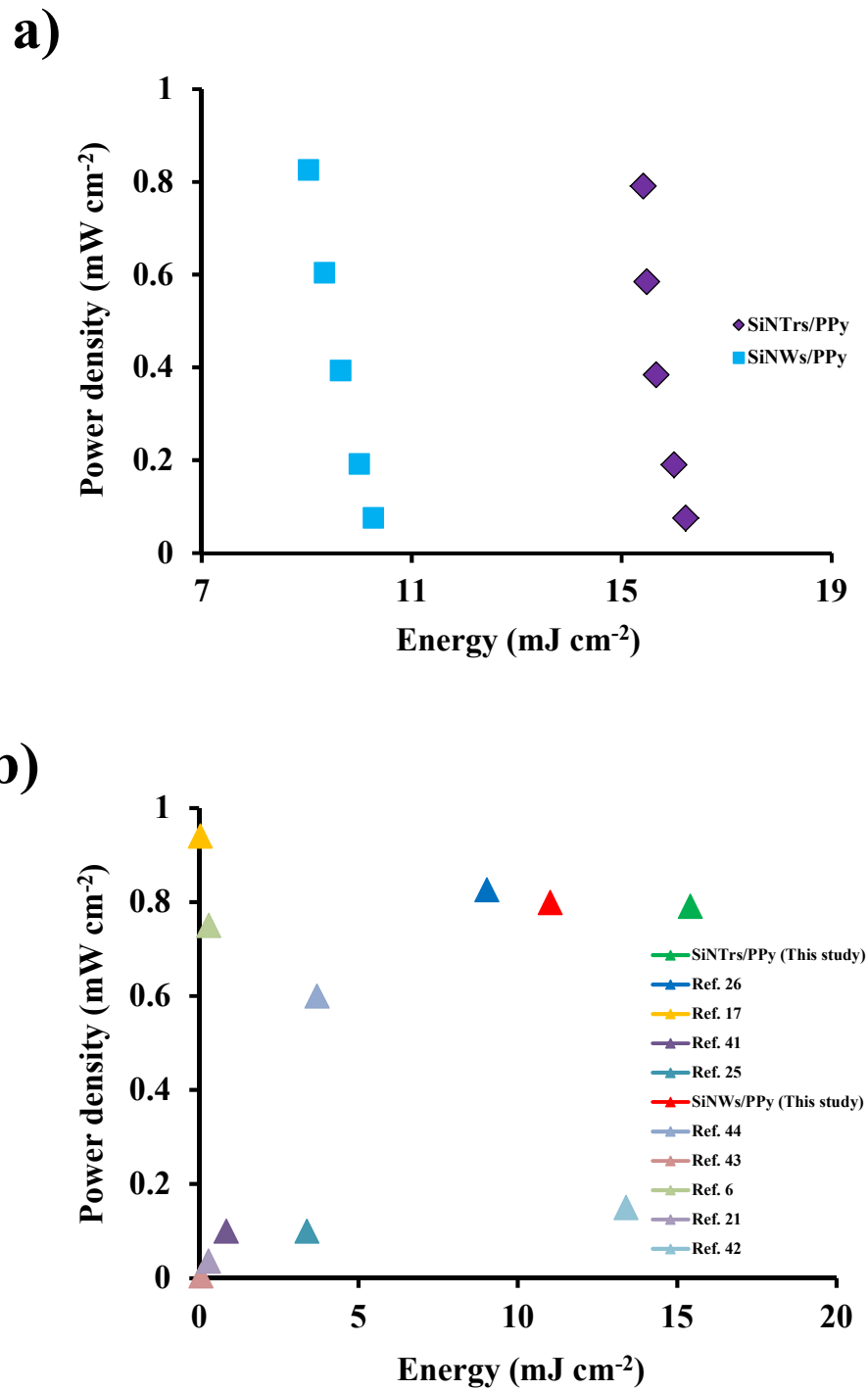


Figure 4

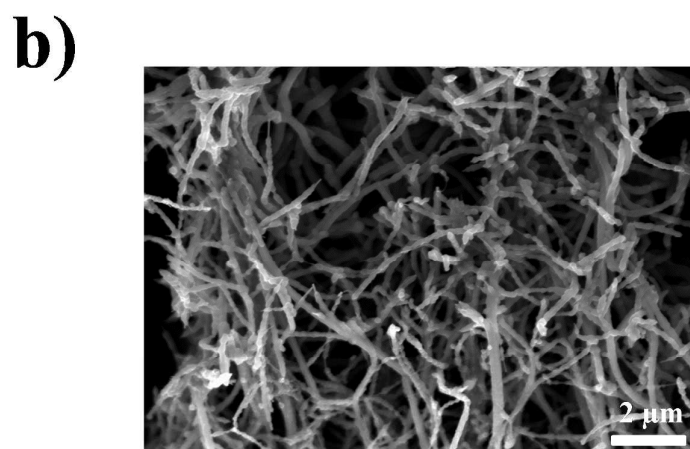
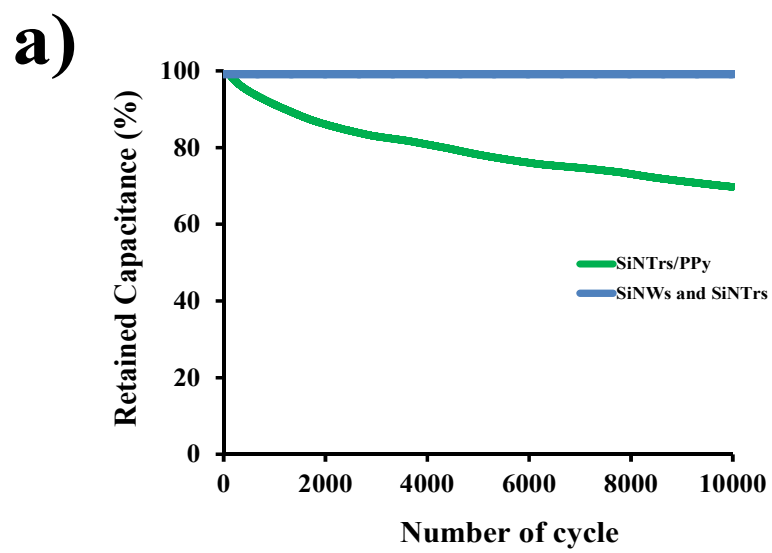
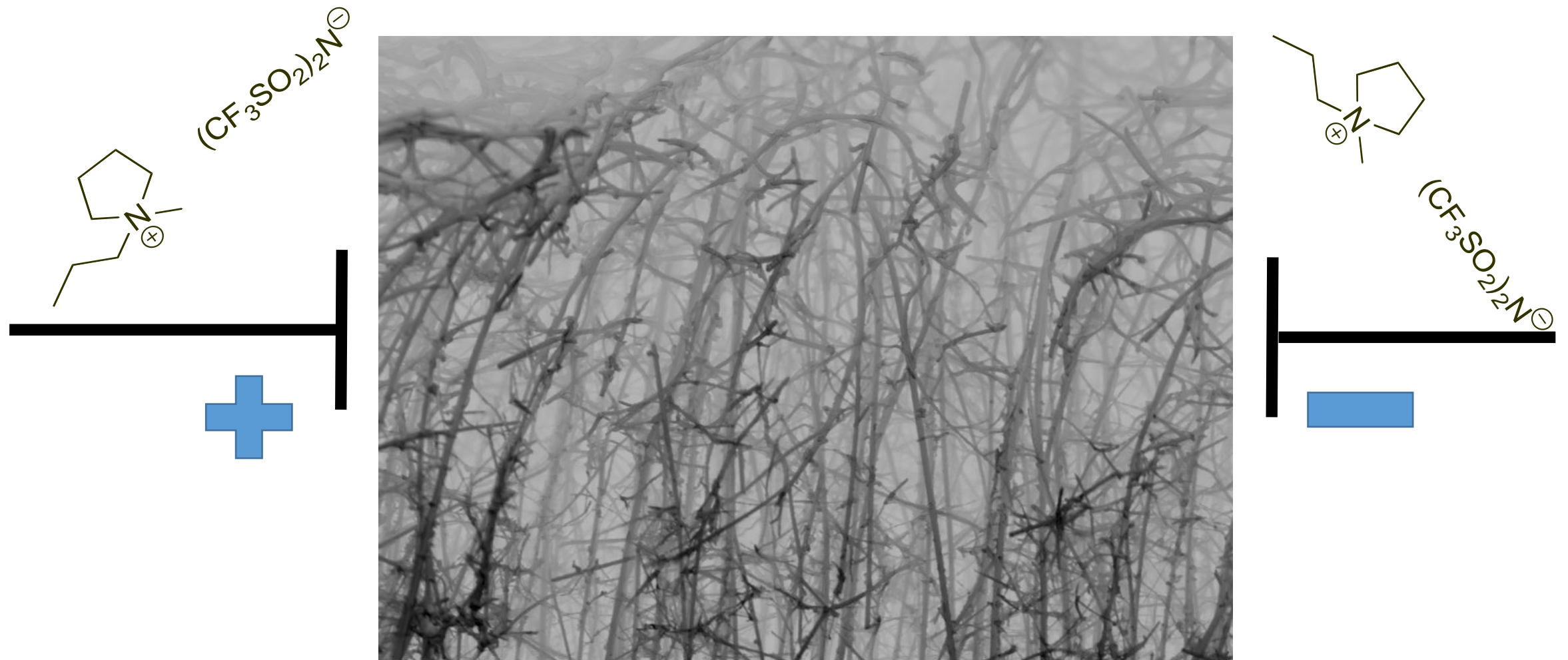


Figure 5



Micro-supercapacitor electrode made of polypyrrole coated silicon nanotrees